A 3D printed photoreactor for investigating variable reaction geometry, wavelength, and fluid flow

Review of Scientific Instruments

A 3D printed photoreactor for investigating variable reaction geometry, wavelength, and fluid flow

Cite as: Rev. Sci. Instrum. **93**, 084103 (2022); https://doi.org/10.1063/5.0087107
Submitted: 01 February 2022 • Accepted: 24 July 2022 • Published Online: 29 August 2022

Alexander Riddell, Patric Kvist and Diana Bernin

A 3D printed photoreactor for investigating variable reaction geometry, wavelength, and fluid flow

Cite as: Rev. Sci. Instrum. 93, 084103 (2022); doi: 10.1063/5.0087107
Submitted: 1 February 2022 • Accepted: 24 July 2022 •
Published Online: 29 August 2022

Alexander Riddell,[a] Patric Kvist, and Diana Bernin

AFFILIATIONS

Department of Chemistry and Chemical Engineering, Chalmers University of Technology, Kemigården 4, 41296 Gothenburg, Sweden

[a]Author to whom correspondence should be addressed: riddell@chalmers.se

ABSTRACT

Research in the field of photochemistry, including photocatalysis and photoelectrocatalysis, has been revitalized due to the potential that photochemical reactions show in the sustainable production of chemicals. Therefore, there is a need for flexible photoreactor equipment that allows for the evaluation of the geometry, light wavelength, and intensity of the vessel, along with the fluid flow in various photochemical reactions. Light emitting diodes (LEDs) have narrow emission spectra and can be either pulsed or run continuously; being flexible, they can be arranged to fit the dimensions of various types of the reactor vessel, depending on the application. This study presents a 3D printed photoreactor with the ability to adjust distances easily and switch between high-power LED light sources. The reactor design utilizes customized printed circuit boards to mount varying numbers and types of LEDs, which enables multiple wavelengths to be used simultaneously. These LED modules, comprised of heat sinks and cooling fans, fulfill the higher heat dissipation requirements of high-power LEDs. The flexibility of the reactor design is useful for optimizing the reaction geometry, flow conditions, wavelength, and intensity of photochemical reactions on a small scale. The estimates for incident light intensity under five possible reactor configurations using ferrioxalate actinometry are reported so that comparisons with other photoreactors can be made. The performance of the photoreactor for differing vessel sizes and distances, in both the flow and batch modes, is given for a photochemical reaction on 2-benzyloxyphenol—a model substance for lignin and applicable in the production of biobased chemicals.

I. INTRODUCTION

Increased interest in photochemistry, photocatalysis and photoelectrocatalysis, has been generated in recent years due to the potential of photochemical reactions for several reasons: their high selectivity, their ability to operate close to ambient temperature and pressure, and the avoidance of additional chemical reagents.[1–3] Chemical processes driven by high-power light-emitting diodes (LEDs) could be advantageous both in terms of energy efficiency and operating flexibility. The use of electricity to power LEDs as the main driver of chemical reactions aligns with the "Power-to-Chemicals" concept, which aims at achieving stability of the electricity grid and sustainability through electrification.[4]

During the early stages of photochemical research, setting up an appropriate photoreactor can seem daunting and the cost of a photochemical reactor setup can be financially challenging. Therefore, a basic understanding of a photochemical system and its experimental requirements is desirable before a larger investment is made. Questions that require consideration include, for example, the kind of reactor that would be the most suitable (batch or flow) and its dimensions; the appropriate wavelength, or combination of wavelengths, along with the light intensity necessary to achieve the desired rates of change. Moreover, the requirements for stirring, flow rate, and control of the reaction atmosphere must also be taken into account.

The 3D printed photoreactor apparatus presented in this paper has length adjustment and the ability to switch easily between different LED light sources. It has an open design and various reactor shapes, sizes, and stirring methods can be run using the same equipment. Well-controlled comparisons can be made between the

reactor settings because the light module distances are fixed on the rails. Actinometry can be employed to characterize the incident light intensity in different reactor setups, thereby enabling comparisons between reactor geometries to be made. The cooling requirements of high-power LEDs are satisfied by attaching electric fans to each light module separately: the LEDs are, thus, cooled sufficiently while remaining mobile.

Although laboratory-scale batch, flow and micro photoreactors currently exist on the market, they are typically not flexible enough for testing multiple reaction setups with the same apparatus. However, it has been demonstrated already that 3D printing and LEDs can produce photoreactors that are low-cost and can be tailored to meet specific needs, such as wastewater treatment, chemical conversion, and particle synthesis.[5–8] Other laboratory-scale photoreactors focus on controlling the distribution of incident wavelengths, homogeneity of photon flux, and intensified mass transport.[9]

The integration of LEDs, heat sinks, and cooling fans into modules that can be easily moved and exchanged form a very useful feature of the design presented here. The use of high-power LEDs requires additional cooling due to their heat dissipation. Temperature control is important because there is a decrease in the intensity and an increase in the emitted wavelength with the increasing temperature; adjusting the location of light sources in a reactor with cooling fans fixed into place is difficult. A combination of various light modules or customized printed circuit boards can be used to test the effects of using LEDs of more than one wavelength: this would be relevant if there were more than one photoactivated process of interest that required different photon energies. An explanation of the features of this reactor, and an example of incident light intensity estimation using ferrioxalate actinometry, are described here, with STL files of the reactor parts included for easy printing and adaptation. The photoreactor is demonstrated in both flow and batch modes in a photochemical reaction breaking an ether bond in the model substance, 2-benzyloxyphenol (2BP).

II. MATERIALS AND METHODS

A. Photoreactor

The following LEDs were used: DUV 280 SD356 (Roithner Lasertechnik GmbH, Vienna, Austria), CIS_Klaran_WD_DS-07142019 (Crystal IS USA), and XST-3535-UV-A60-CE280-01 (Mouser Electronics, USA). The printed circuit boards were either bought from Roithner Lasertechnik GmbH, Vienna, Austria, or designed and submitted for printing. The LEDs were run using a power supply of 50 V max.

A heat sink—PGA 14 K/W (Fischer Elektronik)—was used, along with an axial fan—DC 40 × 40 × 10 mm^3 5 V 14 m^3/h (Sunon). The fans were run on a 5 V power supply.

The flow loop (10 ml replacement UV-150 reactor tubing 50-1581) was sourced from Vapourtec, UK, the flow speed of which was adjusted with a Watson Marlow 505S Manual Drive, 220RPM pump.

Polylactic acid (PLA) (glass transition range 60–65 °C; melting range 173–178 °C) was used for the 3D printing of the photoreactor components. The 3D printer used was a filament printer (Creality ender-3 v2) with a printing temperature of 200 °C and a bed temperature around 60 °C.

All CAD designs were made in Fusion 360 (Autodesk, Inc.). The STL files can be found in the supplementary material.

B. Chemicals

The following chemicals were used as received: acetonitrile 99.5% (Sigma-Aldrich); iron sulfate $FeSO_4$ 97%, 1,10-phenanthroline, potassium oxalate monohydrate 99%, and 2-(benzyloxy)phenol 96% (Sigma-Aldrich); Acetonitrile-dand chloroform-D1, 0.03 vol. % TMS, deuteration degree min, 99.8% (Merck).

C. Photochemical reactions

Reactions of 1 g/l and 10 g/l 2-benzyloxyphenol (2BP) in acetonitrile were performed to demonstrate the use of the batch and flow setups of the photoreactor. The volume of solution was 50 ml for flow, and 30 and 50 ml for batch. For the batch reaction, parafilm was used to cover the quartz beaker to prevent absorption of water by acetonitrile; for the flow reaction, the pump was set to 23 rotations/min and all contents were closed off from the atmosphere. Samples were taken at time intervals of 0, 15, 30, and 60 min.

D. Nuclear magnetic resonance (NMR)

The samples were transferred to a 3 or 5 mm nuclear magnetic resonance (NMR) tube and 50–100 μl of chloroform-D1 was added. ^{1}H NMR spectra were recorded on a Bruker Avance III HD (700 MHz ^{1}H) equipped with a QCI cryoprobe; the temperature was set to 25 °C. The ^{1}H 1D spectra were collected with a repetition delay of 15 s and the signal was accumulated 128 times. The acetonitrile peak at 1.98 ppm was suppressed using the single solvent suppression watergate technique.[10]

III. THE REACTOR

The reactor consists of seven 3D printed components: a base and two parts for each of the three light source modules, as shown in Fig. 1. The light source modules, henceforth referred to as LED modules, are composed of two 3D printed components screwed together to hold the heat sink and fan [Fig. 1(a)]. The surface available on the heat sink is ~30 × 30 mm^2, and a cooling fan is attached to the back of each module [Fig. 1(a)]—fans are necessary because the high-power LEDs dissipate roughly 4–5 W of heat each during operation. The LED modules are then inserted into the three sets of rails/tracks at the base, as illustrated in Fig. 1(b): their distance from the center can thereby be easily adjusted by sliding them along the rails. The thickness of the base, which is 10 mm here, enables both overhead and magnetic stirring. In the flow mode, the reactor vessel is closed and, thus, allows the atmosphere to be controlled, whereas in the batch mode, the reaction vessels are accessible from the top.

The adjustable distance between the center and the surface of each LED module is 15–65 mm with this photoreactor setup. The STL files (see supplementary material) can be used to adapt the range to any other range—the one used here allowed changes to be made in the vessel geometries, including UV-transparent quartz beakers for batch reactors and UV-transparent polymer tubing for flow reactors.

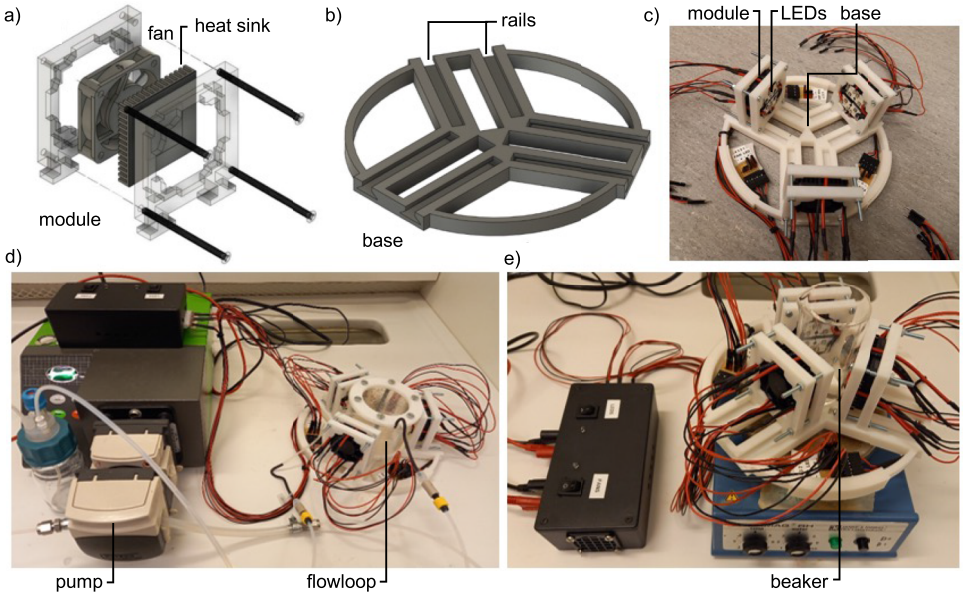

FIG. 1. Images of a module (a) and the base (b) of the photoreactor (d) and (e). LED modules can slide along the three rails/tracks (c). This base can be placed on a heating/stirring device (e).

A completely assembled photoreactor is shown in Fig. 1(c), while Figs. 1(d) and 1(e) show the reactor configured as a flow reactor and a batch reactor, respectively.

A. Choice of wavelength and LED

Other wavelengths, or a combination of wavelengths, can be introduced quickly by switching the LED modules. It may be necessary to use different wavelengths if a sequence of photochemical reactions occurs in which different reactants respond in dissimilar ways to different wavelengths. Moreover, LEDs that have lost intensity or broken down can be adjusted easily by swapping to another LED module. Designing a customized circuit board, an example of which is shown in Fig. 2, allows not only an unlimited combination of different wavelengths to be used but also irradiation to be optimized. LEDs are produced with a range of wavelengths and similar power consumption—they are available with different lenses that provide a narrow or wide-angle light distribution, which enables further customization of the light intensity reaching the reactor vessel. The corresponding footprints of LEDs are often provided by the manufacturer, which makes designing the printed circuit board simple. The printed circuit board is mounted onto the heat sink with either a heat-conducting adhesive or a heat-conducting paste. The board shown in Fig. 2 has two circuits with four LEDs, each connected in series; each module has a resistor to ensure an equal current flowing through each LED. All experiments were run with the LEDs turned on. However, LEDs do permit fast-switching and pulsing to take place, something that might not be possible with other light sources.

B. Ferrioxalate actinometry

The intensity of photoreactors is often reported in terms of the power consumption of the light source. However, this value is inaccurate for estimating the light intensity that reaches the reaction volume (incident light intensity) because some of the light emitted by the source is lost due to reflection and some misses the vessel entirely. Therefore, chemical actinometry is used to obtain a more accurate estimate of incident light intensity, which measures a change in color of a so-called actinometer solution that changes color as photons are absorbed. The actinometer solution is irradiated in the reaction vessel for a measured time, and the absorbance difference at 510 nm between the irradiated and non-irradiated solution is measured with UV–vis. The incident light intensity can thereafter be calculated based on the change in the absorbance value and the irradiation time. The use of actinometry is important

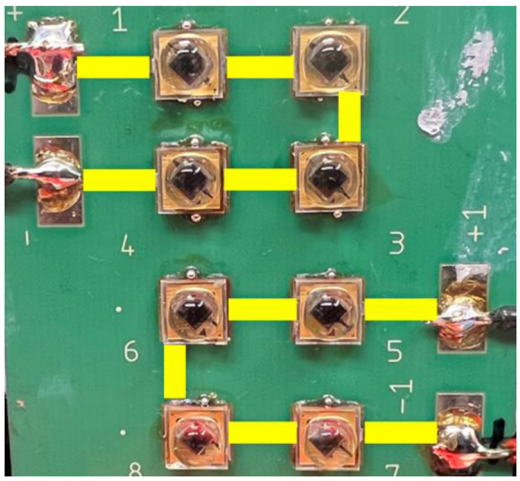

FIG. 2. Customized printed circuit board for eight LEDs mounted on a heat sink with heat-conducting paste. The circuit of the LEDs connected in series is highlighted in yellow.

TABLE I. Results of ferrioxalate actinometry of the two reactor setups (flow and batch) and modules.

Reactor	Setup	Wavelength (nm)	Total current (A)	Intensity ($\times 10^{-5}$ mol photons l^{-1} s^{-1})
12 LEDs	Flow	280	5	3.1
12 LEDs	Batch	265	5	2.0
12 LEDs	Batch	280	5	2.1
24 LEDs	Flow	280	3	9.5
24 LEDs	Batch	280	3	8.3

because inconsistency in characterizing setups has led to issues in reproducibility in the field of photochemistry.[11] Ferrioxalate actinometry is the most commonly used method, and was carried out according to the procedure of Murov *et al.*[12]—based on ideal cases in the literature, these actinometry measurements would have an error of at least 10%.[13] The LEDs used here emit UV light, which is invisible to the naked eye; therefore, they emit some visible light to indicate that they are turned on. The ferrioxalate actinometer reacts with both UV and visible light, so the estimation of incident light intensity is affected by the light from the indicator. However, the comparison between the reactor setups remains valid. The actinometry results obtained for the various reactor setups used are summarized in Table I.

Reactions using 265 nm LEDs cannot be performed in the flow reactor due to absorbance by the polymer tubing. The geometry of the reactor vessel affects the percentage of light that reaches the reaction volume from the LEDs—the intensity of the light within two different containers may differ despite the intensity of its source being the same. The measurements of light intensity reported in Table I met expectations, i.e., the batch modes produced a similar incident light intensity. The milder curves and larger area of the flow reactor vessel resulted in a slightly larger incident light intensity than the batch reactor vessel, as these led to more photons entering the reaction volume.

A higher incident light intensity was measured for the setup with 24 LEDs compared to 12 LEDs. This is, of course, expected as a greater intensity of light is emitted by the LEDs in total. The type of LEDs used for the 24 LED setup also emits a narrower beam of light because the light is focused with lenses; however, less light is lost due to it missing the reaction vessel completely.

IV. RESULTS

A. Batch vs flow

The two different photoreactor modes, i.e., flow (red) and batch (blue and gray), were demonstrated by the photochemical reaction of the model substance, 2BP (1 g/l), and monitored using ^{1}H nuclear magnetic resonance (NMR) (see Fig. 3). All reactions were performed with the 24 LED setup at the closest possible distance. The ^{1}H NMR spectrum of 2BP in acetonitrile at 0 h is shown in Fig. 3(a). The spectra after 1 h of reaction time [Fig. 3(b)] for the flow (red), batch 50 ml (blue), and batch 30 ml (gray) are visually very similar—an observation that is reflected in the decrease of the integral of the ether bond [Fig. 3(c)] with time. This is in

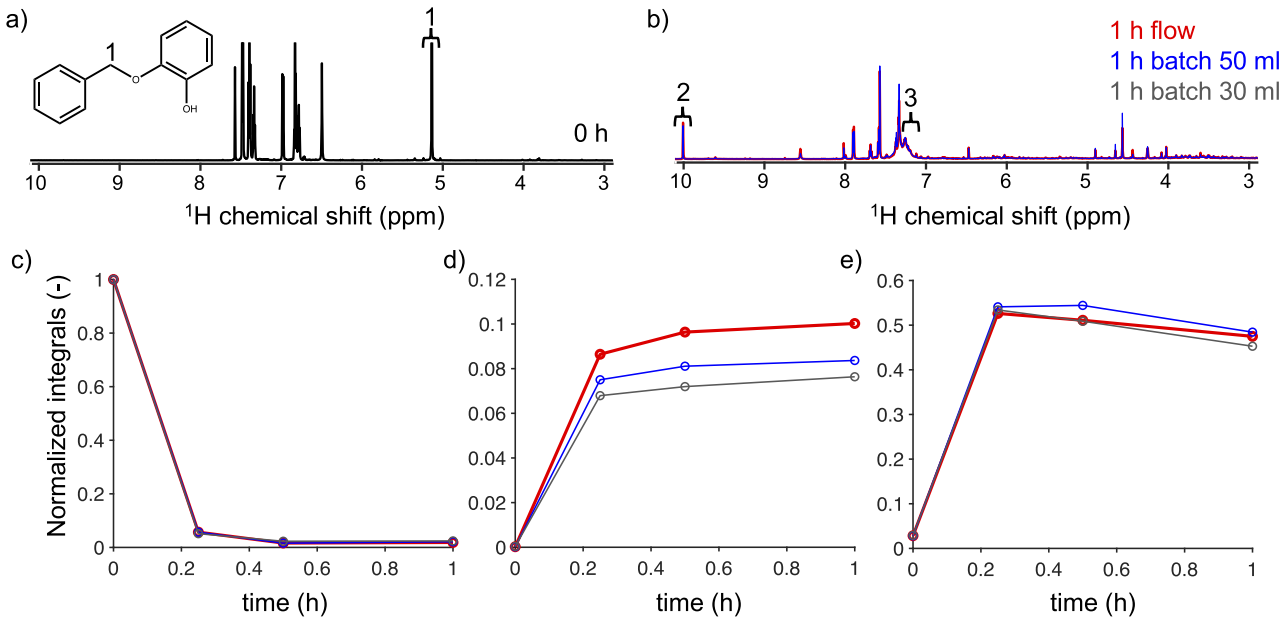

FIG. 3. Photochemical reaction of 1 g/l 2BP in acetonitrile as shown in (a), using the photoreactor setup with 24 LEDs. ^{1}H NMR spectra are shown at 0 h (a) and 1 h (b) for flow (red), batch 50 ml (blue), and batch 30 ml (gray). The reaction progress was monitored by taking the integrals of the peaks labeled 1, 2, and 3 in (a) and (b). The integrals with time correspond to the ether linkage (c), aldehyde group (d), and aromatic group (e).

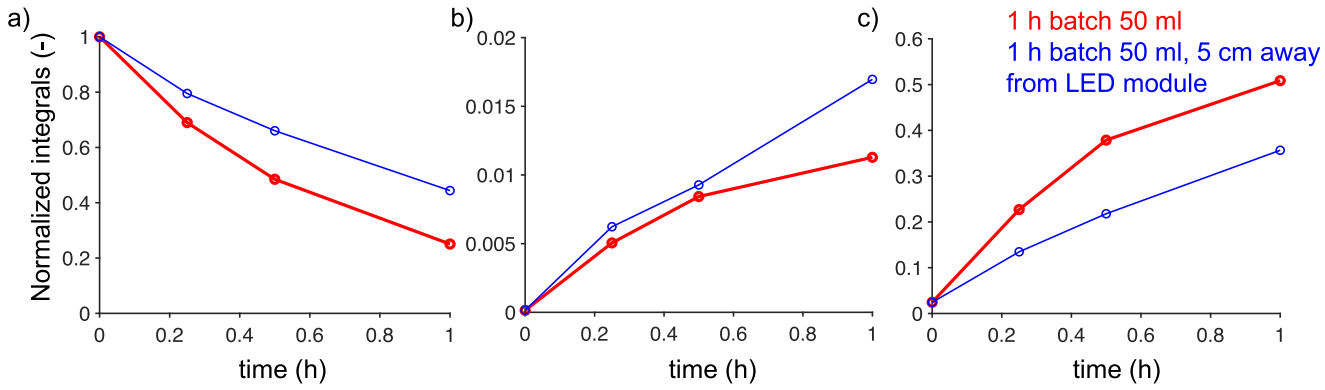

FIG. 4. Photochemical reaction on 10 g/l 2BP in acetonitrile using the 24 LED flow photoreactor setup. Integrated intensity values taken from ^{1}H NMR peaks are shown from 0 to 1 h for 50 ml batch (red) and 50 ml batch placed 5 cm from the LED module (blue). The progress of the reaction was monitored by taking the integrals of the ^{1}H NMR peaks highlighted with 1, 2, and 3 in Figs. 3(a) and 3(b). The integrals correspond to the ether linkage (a), aldehyde group (b), and aromatic group (c).

agreement with Hynynen *et al.*,[14] who reported on the cleavage of the ether bond in 2BP upon irradiation. All ether bonds are almost completely cleaved after 15 min regardless of the photoreactor mode. Corcoran *et al.*[15] observed similar reaction yields in both batch and flow modes.

A difference in the integral vs time is monitored for the aldehyde formation for the flow (red), batch 50 ml (blue), and batch 30 ml (gray), as shown in Fig. 3(d), while the formation of the aromatic group is comparable. It is important to note that the flow reactor produces a higher incident light intensity (Table I) than the quartz beaker batch reactor. However, it is possible that the difference in the light intensity does not explain the similar progression of the reaction. It is well known that mass transport caused by mixing may affect a photochemical reaction and byproducts may be formed due to local concentration gradients.[16] The mixing that occurred in the photoreactor setups differed, which might have caused the dissimilarity in the formation of aldehyde. (The details of the reaction kinetics and molecules formed are beyond the scope of this paper.)

B. Distance dependence

Figure 4 shows the NMR results of the same reaction (10 g/l 2BP) performed in 50 ml batch mode with the LED modules placed 5 cm away from the beaker: as expected, the rate of cleavage of the ether linkage is slower [Fig. 4(a)]. This is also true for the formation of the aromatic group [Fig. 4(c)]. In contrast, the formation of aldehyde [Fig. 4(b)] follows the same trend up to 30 min for both setups before deviating at 1 h. There are probably several reasons for this deviation: the reaction may not be driven solely by photons, and the aldehyde formation is caused by other reactions occurring simultaneously.

V. LIMITATIONS

Despite the flexibility and advantages of the photoreactor design presented, there are some areas in which a different apparatus would be more suitable: there are many flow microreactors designed for specific mixing requirements, e.g., to control the size of nanoparticles.[17] Reactor designs with a light source of even intensity at many points would also be preferable for cases where several small reaction vessels are in simultaneous use. Although the narrow emission spectrum of LEDs is an advantage in many experiments, there may be some cases where a broader emission spectrum is desirable, e.g., in mimicking the sun—such LEDs are also available.

VI. CONCLUSION

The expanding field of photoreaction engineering has the potential of contributing positively to meeting several challenges related to sustainability and decarbonization of chemical production. Investigating the performance of photoreactors is complex, partly because the intensity of photons and the concentrations of chemical species are distributed unevenly throughout the volume of the reactor. Whether or not batch reactors, flow reactors, microreactors, etc. are appropriate for a given photochemical reaction is determined by the ways in which the reaction is affected by photon and mass transport. The purpose of the design presented here is to provide a convenient and flexible apparatus for testing the shape and volume of the reactor, mixing method, light wavelength, and light intensity so that the relative influence of these variables can be estimated and the requirements of a future reactor assessed.

SUPPLEMENTARY MATERIAL

See supplementary material for the STL files of the reactor base and light source modules.

ACKNOWLEDGMENTS

The authors thank Prof. Bengt Andersson for his input regarding the photoreactor. They acknowledge funding from *Södras forskningsstiftelse* (Grant Nos. 2019-102 and 2020-168) and Swedish Research Council (Grant No. 2019-04066).

AUTHOR DECLARATIONS

Conflict of Interest

The authors have no conflicts to disclose.

Author Contributions

Alexander Riddell: Conceptualization (equal); Data curation (equal); writing – original draft (equal); writing – review & editing (equal). **Patric Kvist**: Conceptualization (equal); Supervision (equal). **Diana Bernin**: Conceptualization (equal); Formal analysis (equal); Funding acquisition (equal); Methodology (equal); Project administration (equal); Supervision (equal); writing – original draft (equal); writing – review & editing (equal).

DATA AVAILABILITY

The data that support the findings of this study are available from the corresponding author upon reasonable request.

REFERENCES

[1]C. A. Clark, D. S. Lee, S. J. Pickering, M. Poliakoff, and M. W. George, "A simple and versatile reactor for photochemistry," Org. Process Res. Dev. **20**(10), 1792–1798 (2016).

[2]J. D. Williams and C. O. Kappe, "Recent advances toward sustainable flow photochemistry," Curr. Opin. Green Sustainable Chem. **25**, 100351 (2020).

[3]L. Buglioni, F. Raymenants, A. Slattery, S. D. A. Zondag, and T. Noël, "Technological innovations in photochemistry for organic synthesis: Flow chemistry, high-throughput experimentation, scale-up, and photoelectrochemistry," Chem. Rev. **122**(2), 2752–2906 (2021).

[4]K. van Kranenburg, E. Schols, H. Gelevert, R. de Kler, Y. van Delft, and M. Weeda, "Empowering the chemical industry: Opportunities for electrification," ECN White Paper, 2016.

[5]L. Zhang, Z. Zhu, B. Liu, C. Li, Y. Yu, S. Tao, and T. Li, "Fluorescent fluid in 3D-printed microreactors for the acceleration of photocatalytic reactions," Adv. Sci. **6**, 1900583 (2019).

[6]S. Rossi, M. V. Dozzi, A. Puglisi, and M. Pagani, "3D-printed, home-made, UV-LED photoreactor as a simple and economic tool to perform photochemical reactions in high school laboratories," Chem. Teach. Int. **2**(2), 20190010 (2019).

[7]S. J. Phang, V.-L. Wong, K. H. Cheah, and L.-L. Tan, "3D-printed photoreactor with robust g-C_3N_4 homojunction based thermoset coating as a new and sustainable approach for photocatalytic wastewater treatment," J. Environ. Chem. Eng. **9**, 106437 (2021).

[8]S. Ponce, M. Hernandez, K. Vizuete, D. A. Streitwieser, and A. Debut, "Fast synthesis of silver colloids with a low-cost 3D printed photo-reactor," Colloids Interface Sci. Commun. **43**, 100457 (2021).

[9]E. Kayahan, M. Jacobs, L. Braeken, L. C. J. Thomassen, S. Kuhn, T. van Gerven, and M. Enis Leblebici, "Dawn of a new era in industrial photochemistry: The scale-up of micro- and mesostructured photoreactors," Beilstein J. Org. Chem. **16**, 2484–2504 (2020).

[10]M. Piotto, V. Saudek, and V. Sklenář, "Gradient-tailored excitation for single-quantum NMR spectroscopy of aqueous solutions," J. Biomol. NMR **2**, 661–665 (1992).

[11]H. E. Bonfield, T. Knauber, F. Lévesque, E. G. Moschetta, F. Susanne, and L. J. Edwards, "Photons as a 21st century reagent," Nat. Commun. **11**, 804 (2020).

[12]S. L. Murov, I. Carmichael, and G. L. Hug, *Handbook of Photochemistry*, 2nd ed. Revised and Expanded ed. (Marcel Dekker, 1993), pp. 300–305.

[13]T. Lehóczki, É. Józsa, and K. Ősz, "Ferrioxalate actinometry with online spectrophotometric detection," J. Photochem. Photobiol., A **251**, 63–68 (2013).

[14]J. Hynynen, A. Riddell, A. Achour, Z. Takacs, M. Wallin, J. Parkås, and D. Bernin, "Lignin and extractives first conversion of lignocellulosic residual streams using UV light from LEDs," RSC Green Chem. **23**, 8251–8259 (2021).

[15]E. B. Corcoran, J. P. McMullen, F. Lévesque, M. K. Wismer, and J. R. Naber, "Photon equivalents as a parameter for scaling photoredox reactions in flow: Translation of photocatalytic C–N cross-coupling from lab scale to multikilogram scale," Angew. Chem., Int. Ed. **59**, 11964–11968 (2020).

[16]D. Cambié, C. Bottecchia, N. J. W. Straathof, V. Hessel, and T. Noël, "Applications of continuous-flow photochemistry in organic synthesis, material science, and water treatment," Chem. Rev. **116**, 10276–10341 (2016).

[17]X. Yao, Y. Zhang, L. Du, J. Liu, and J. Yao, "Review of the applications of microreactors," Renew. Sust. Energ. Rev., **47**, 519–539 (2015).